

Electrical Breakdown of a Metallic Nanowire Mesh

Yuan Li^{1,*}, Kaoru Tsuchiya¹, Hironori Tohmyoh¹, Masumi Saka¹

¹ Department of Nanomechanics, Tohoku University, Sendai 980-8579, Japan

* Corresponding author: liyuan@ism.mech.tohoku.ac.jp

Abstract The electrical breakdown of a metallic nanowire mesh induced by Joule heating (i.e., melting) is investigated by solving the corresponding electro-thermal problem, where the effect of electromigration is neglected. A numerical computational program is firstly developed to simulate the temperature profile for a metallic wire mesh and investigate the melting current triggering the melting of mesh segment. The melting process of the mesh structure is investigated by analyzing the variation of melting current with regard to the melting propagation of mesh segment. On this basis, the melting behavior of a system of the mesh equipped with current source is predicted. For both current-controlled and voltage-controlled current source, local instability (i.e., at a constant current/voltage, several mesh segments melt simultaneously) and stable melting (i.e., the increase of current/voltage is necessary for the melting of mesh segment) will happen. Moreover, global instability (i.e., at a constant current, several mesh segments melt until the circuit of mesh opens) will occur only at the mode of current-controlled current source.

Keywords Electrical breakdown, Instability, Joule heating, Metallic nanowire mesh, Stable melting,

1. Introduction

With one-dimensional structure and nanometer-scale diameter, metallic nanowires have shown remarkable electrical, mechanical, optical and chemical properties [1]. Successful assembly of these metallic nanowires into a mesh structure has offered great potential as components for large-scale integrated devices in nanoelectronics and photonics. Recent reports have shown that such mesh can play new roles which are far from the potential of individual nanowires, including transparent conductors, low-cost flexible electronics [2, 3]. It is well known that if an electrically conductive material is subjected to current flow, Joule heating occurs [4]. Joule heating in these metallic nanowires may go beyond degrading the electrical performance of the corresponding metallic nanowire mesh, and therefore deteriorate the reliability of the mesh-based devices. In order to turn around this problem, clarifying the electrical breakdown of a metallic nanowire mesh induced by Joule heating becomes urgent. Up to date, the electrical breakdown of an individual metallic nanowire has been investigated systematically including melting due to Joule heating [5, 6] and due to electromigration [7-10]. The former has been used to cut metallic nanowire in any desirable length [5, 6] for specific purpose, and the latter has been employed to make the nanogap [7, 8] between metal electrodes into which individual molecules can be inserted to measure their electrical properties. However, little is currently known regarding the electrical breakdown of a metallic nanowire mesh, which is expected to show different characteristics because of its unique mesh structure.

In this work, the electrical breakdown of a metallic nanowire mesh induced by Joule heating (i.e., melting) is investigated for the first time. To deal with this type of electro-thermal problem, a numerical simulation method is proposed to determine the associated temperature field for a metallic wire mesh and the variation of the melting current triggering the melting of mesh segment with the melting propagation of mesh segment. By employing the developed computational program, the melting process of a silver (Ag) nanowire mesh structure is clarified by analyzing the variation of melting current during the melting propagation in the mesh. It then indicates the interesting characteristics of the melting behavior for a system of the mesh equipped with current source.

2. Simulation Method for Electrical Breakdown of a Metallic Nanowire Mesh

2.1 Simulation Model and Basic Assumptions

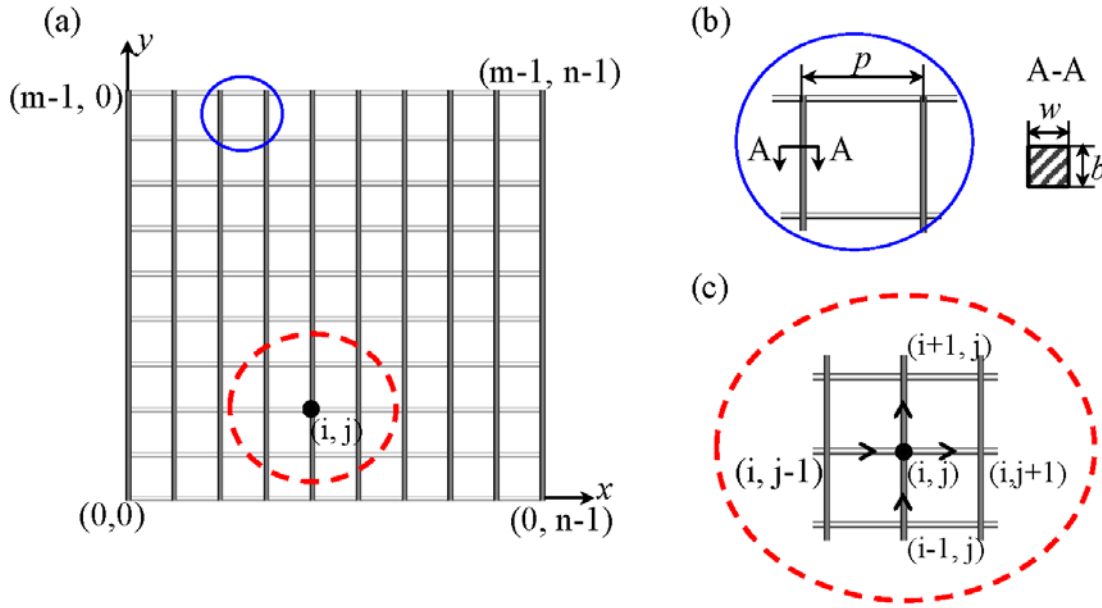


Fig. 1 Schematic illustration of a metallic nanowire mesh ($m \times n$)

A metallic nanowire mesh with size of $m \times n$ is schematically illustrated in Fig. 1, which is a uniform rectangular grid of wires with m rows (horizontal wires) and n columns (vertical wires). As shown in Fig.1b, the pitch size is p , the wire width and thickness are w and b , respectively. Due to the complex nature of electro-thermal for a metallic wire mesh, the following assumptions are made: (1) The material of metallic mesh is homogeneous and isotropic; (2) Material properties of metallic mesh are temperature independent; (3) The effect of electromigration is neglected for simplicity.

2.2 Fundamentals of Governing Equations

A mesh node is an intersection of each row and column. Let node (i, j) be the intersection of the $(i+1)^{\text{th}}$ row and the $(j+1)^{\text{th}}$ column, where $i=0, \dots, m-1$; $j=0, \dots, n-1$. The wire between two adjacent mesh nodes is called a mesh segment. For the present mesh with size of $m \times n$, the numbers of mesh nodes and mesh segments are $m \times n$ and $m(n-1) + n(m-1)$, respectively. The segment between node $(i, j-1)$ and node (i, j) is denoted as $s_{i,j}^l$, and the segment between (i, j) and $(i, j+1)$ is denoted as $s_{i,j}^r$. Similarly, the segment between node $(i-1, j)$ and (i, j) is denoted as $s_{i,j}^d$, and the segment between (i, j) and $(i+1, j)$ is denoted as $s_{i,j}^u$. Here, the letters of l, r, d and u stand for the relative positions of the adjacent nodes (i.e., $(i, j-1)$, $(i, j+1)$, $(i-1, j)$, $(i+1, j)$) to node (i, j) , i.e., left, right, down, up, respectively.

For any mesh segment, the current can be calculated using Ohm's law. By considering the node (i, j) , the current flowing between four adjacent nodes and it can be obtained as below

$$\begin{aligned}
 I_{S_{i,j}^l} &= j_{S_{i,j}^l} A = -\frac{1}{\rho} \frac{U_{(i,j)} - U_{(i,j-1)}}{x_{(i,j)} - x_{(i,j-1)}} A \\
 I_{S_{i,j}^r} &= j_{S_{i,j}^r} A = -\frac{1}{\rho} \frac{U_{(i,j+1)} - U_{(i,j)}}{x_{(i,j+1)} - x_{(i,j)}} A \\
 I_{S_{i,j}^d} &= j_{S_{i,j}^d} A = -\frac{1}{\rho} \frac{U_{(i,j)} - U_{(i-1,j)}}{y_{(i,j)} - y_{(i-1,j)}} A
 \end{aligned}$$

$$I_{S_{i,j}^u} = j_{S_{i,j}^u} A = -\frac{1}{\rho} \frac{U_{(i+1,j)} - U_{(i,j)}}{y_{(i+1,j)} - y_{(i,j)}} A \quad (1)$$

where ρ is the electrical resistivity of material, and $A (=wb)$ is the cross-sectional area of wire. Here, as an example, $I_{S_{i,j}^l}, j_{S_{i,j}^l}$ are current and current density for mesh segment $S_{i,j}^l$; $U_{(i,j)}$ and $x_{(i,j)}, y_{(i,j)}$ are electrical potential and coordinates of node (i, j) . It should be noted that as shown in Fig. 1, the origin of the coordinate system is set at the bottom left corner of the mesh, i.e., node $(0, 0)$. The x -axis points right and the y -axis points up, both of which are taken to be along the wire. Moreover, at any mesh node of (i, j) , according to Kirchhoff's current law, we have

$$I_{\text{internal}} + I_{\text{external}} = 0 \quad (2)$$

Here, $I_{\text{internal}} (= I_{S_{i,j}^l} - I_{S_{i,j}^r} + I_{S_{i,j}^d} - I_{S_{i,j}^u})$ means the sum of the current flowing into the node (i, j) from different adjacent nodes, and I_{external} represents the external input/output current where the external output current takes the minus value. By considering Eqs. (1) and (2) for all the nodes, the current density at any mesh segment (i.e., $j_{S_{i,j}^l}, j_{S_{i,j}^r}, j_{S_{i,j}^d}, j_{S_{i,j}^u}$), and the electrical potential at any mesh node can be obtained.

On the other hand, for any mesh segment, the heat energy, flowing in any mesh segment between two adjacent nodes, can be calculated using Fourier's law of heat conduction as

$$\begin{aligned} Q_{S_{i,j}^l} &= q_{S_{i,j}^l} A = -\lambda \frac{T_{(i,j)} - T_{(i,j-1)}}{x_{(i,j)} - x_{(i,j-1)}} A \\ Q_{S_{i,j}^r} &= q_{S_{i,j}^r} A = -\lambda \frac{T_{(i,j+1)} - T_{(i,j)}}{x_{(i,j+1)} - x_{(i,j)}} A \\ Q_{S_{i,j}^d} &= q_{S_{i,j}^d} A = -\lambda \frac{T_{(i,j)} - T_{(i-1,j)}}{y_{(i,j)} - y_{(i-1,j)}} A \\ Q_{S_{i,j}^u} &= q_{S_{i,j}^u} A = -\lambda \frac{T_{(i+1,j)} - T_{(i,j)}}{y_{(i+1,j)} - y_{(i,j)}} A \end{aligned} \quad (3)$$

where λ is the thermal conductivity of material. Here, as an instance, $Q_{S_{i,j}^l}, q_{S_{i,j}^l}$ are heat energy and heat flux for mesh segment $S_{i,j}^l$; $T_{(i,j)}$ is the temperature at node (i, j) . Moreover, at any mesh node, according to the law of conservation of heat energy, we have

$$Q_{\text{internal}} + Q_{\text{external}} = 0 \quad (4)$$

Here, $Q_{\text{internal}} (= Q_{S_{i,j}^l} - Q_{S_{i,j}^r} + Q_{S_{i,j}^d} - Q_{S_{i,j}^u})$ means the sum of the heat energy flowing into the node (i, j) from different adjacent nodes, and Q_{external} represents the external input/output heat energy where the external output heat energy takes the minus value.

It should be noted that when a metallic nanowire is subjected to a steady direct current flow, Joule heating occurs, which, in turn causes increase in temperature of the wire. For simplicity, it is assumed that there is no heat transfer from the surface of the wire to the ambient, and the time-dependence of temperature can be neglected. Then, the heat conduction in the above four mesh segments can be governed by the following one-dimensional Poisson's equations [11]:

$$\begin{aligned} \lambda \frac{d^2 T_{S_{i,j}^l}}{dx^2} + \rho j_{S_{i,j}^l}^2 &= 0 \\ \lambda \frac{d^2 T_{S_{i,j}^r}}{dx^2} + \rho j_{S_{i,j}^r}^2 &= 0 \\ \lambda \frac{d^2 T_{S_{i,j}^d}}{dy^2} + \rho j_{S_{i,j}^d}^2 &= 0 \\ \lambda \frac{d^2 T_{S_{i,j}^u}}{dy^2} + \rho j_{S_{i,j}^u}^2 &= 0 \end{aligned} \quad (5)$$

where $T_{S_{i,j}^l}$ as an example is the temperature of mesh segment $S_{i,j}^l$.

Using the above Eqs. (3) to (5) for all the nodes, the temperature at any mesh node (i.e., $T_{(i,j-1)}$, $T_{(i,j+1)}$, $T_{(i-1,j)}$, $T_{(i+1,j)}$, $T_{(i,j)}$) can be obtained. For a specific mesh segment, if two ends of it (i.e., two adjacent mesh nodes) have the same temperature, the temperature at its center T^C is also the highest temperature T^{\max} in the mesh segment (i.e., $T^C = T^{\max}$), which can be calculated [11] as

$$\begin{aligned} T_{S_{i,j}^l}^C &= \frac{\rho}{2\lambda} j_{S_{i,j}^l}^2 \left(\frac{x_{(i,j)} - x_{(i,j-1)}}{2} \right)^2 + \frac{T_{(i,j)} + T_{(i,j-1)}}{2} \\ T_{S_{i,j}^r}^C &= \frac{\rho}{2\lambda} j_{S_{i,j}^r}^2 \left(\frac{x_{(i,j)} - x_{(i,j+1)}}{2} \right)^2 + \frac{T_{(i,j)} + T_{(i,j+1)}}{2} \\ T_{S_{i,j}^d}^C &= \frac{\rho}{2\lambda} j_{S_{i,j}^d}^2 \left(\frac{y_{(i,j)} - y_{(i-1,j)}}{2} \right)^2 + \frac{T_{(i,j)} + T_{(i-1,j)}}{2} \\ T_{S_{i,j}^u}^C &= \frac{\rho}{2\lambda} j_{S_{i,j}^u}^2 \left(\frac{y_{(i,j)} - y_{(i+1,j)}}{2} \right)^2 + \frac{T_{(i,j)} + T_{(i+1,j)}}{2} \end{aligned} \quad (6)$$

In the present case, most mesh segments have different temperatures at its ends. In view of the very small length of mesh segment of $200\mu\text{m}$ as shown later in Fig. 3, the temperature at the center of mesh segment is approximately considered as the maximum temperature in mesh segment T^{\max} (i.e., $T^C \approx T^{\max}$). Once the maximum temperature in a mesh segment T^{\max} reaches to the melting point of the material T_m , it is thought that electrical breakdown induced by Joule heating happens at this mesh segment, i.e., this mesh segment melts.

2.3 Computational Procedure

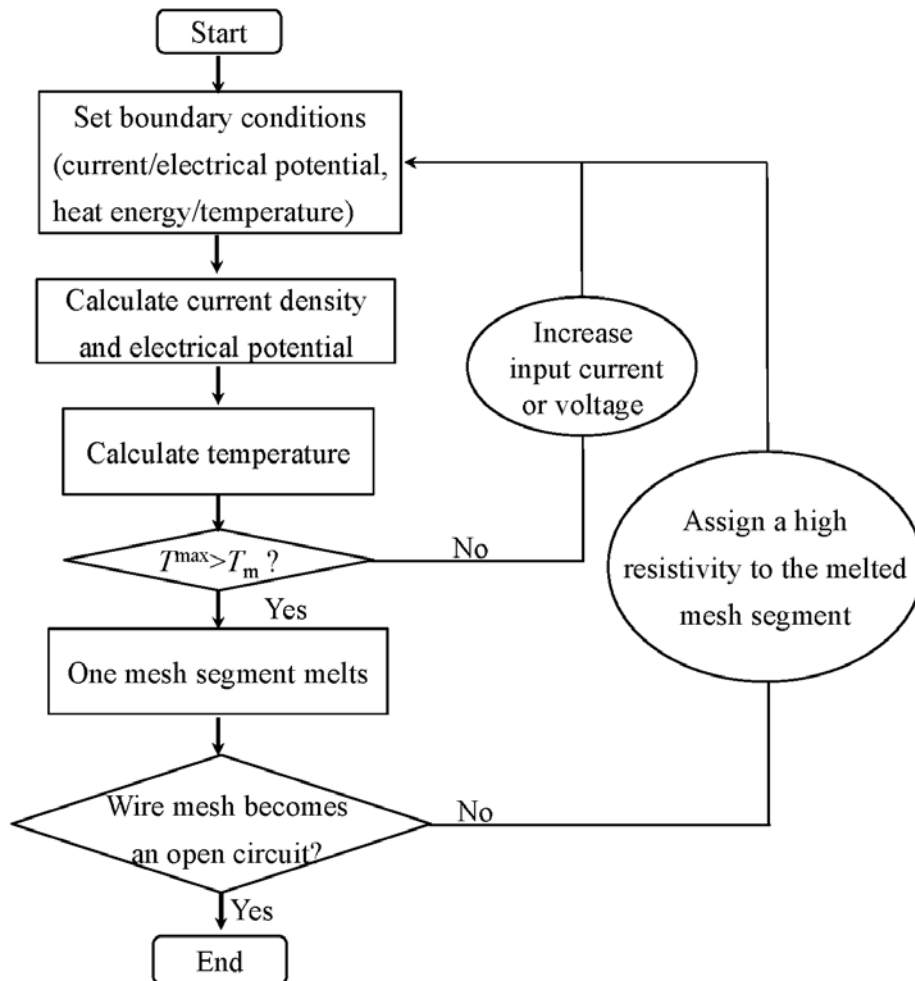


Fig. 2 Flow chart of numerical simulation

A corresponding computational program is developed to solve this electro-thermal problem regarding the electrical breakdown of the metallic nanowire mesh induced by Joule heating. Note that to record precisely the melting current triggering the melting of mesh segment, the increment of current should be tuned to make mesh segment melt one by one. The corresponding simplified flow chart of this program is shown in Fig. 2.

3. Electrical Breakdown of an Ag Nanowire Mesh

3.1 Numerical Model

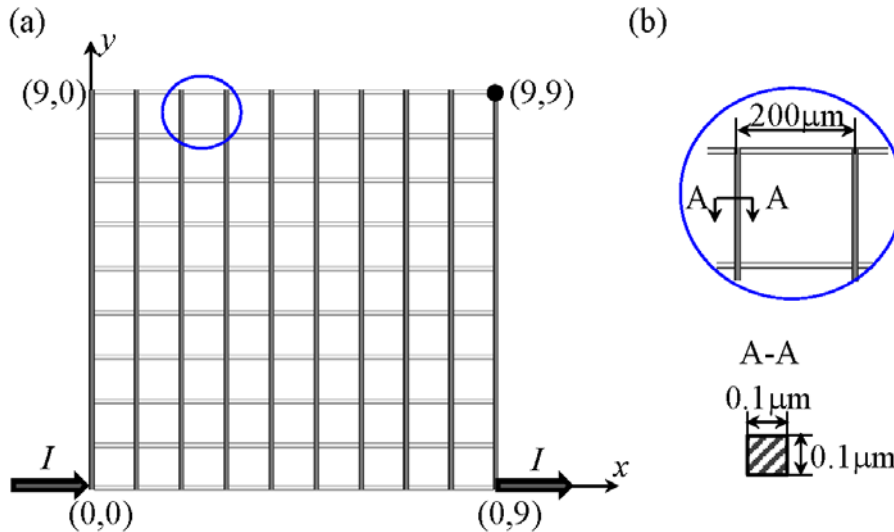


Fig. 3 Schematic illustration of an Ag nanowire mesh (10×10)

Table 1 Physical properties of Ag nanowire

| | |
|---|-----------------------------|
| Melting point T_m (K) | 873 [12] |
| Thermal conductivity λ (W/ $\mu\text{m}\cdot\text{K}$) | 3.346×10^{-4} [13] |
| Electrical resistivity ρ ($\Omega \cdot \mu\text{m}$) | 0.119 [14] |

A silver (Ag) nanowire mesh (10×10) as shown in Fig. 3a is considered here. The numbers of mesh nodes and mesh segments are 100 and 180, respectively. The pitch size is $p=200\mu\text{m}$, both the width and thickness of Ag nanowire are $w=b=100\text{nm}$ as shown in Fig.3b. The physical properties of Ag nanowire are listed in Table 1. Note that size effect on the physical properties is taken into consideration for Ag nanowire.

As shown in Fig. 3a, the external current I flows into the mesh from node (0, 0) and flows out of the mesh from node (0, 9), which means that node (0, 0) has an external input current and node (0, 9) has an external output current. For the other nodes, no any external current is given. A constant value is assigned to the electrical potential of node (9, 9). The temperature of boundary nodes (i.e., (i, 0), (0, j), (i, 9), (9, j) where $i, j=0, \dots, 9$) is room temperature of $T_0=300\text{K}$. There is no any external heat energy for all the other nodes. The developed program is employed to investigate the evolution of the melting current I_m triggering the melting of the mesh segment. Here, in order to make mesh segment melt one by one as much as possible, the increment of the input current is set with a small value of 0.001mA until the melting current is reached. The corresponding melting voltage V_m (i.e., the difference of electrical potential between node (0, 0) and node (0,9)) is also recorded in order to calculate the variation of resistance of the mesh, i.e., R , with regard to the sequential electrical breakdown of mesh segments.

3.2 Results and Discussion

With regard to the melting propagation of mesh segment, the variation of melting current I_m and mesh resistance are shown in Fig. 4a and Fig. 4b. Note that the mesh resistance is the resistance between two mesh nodes where the external current is input and output (i.e., node (0, 0) and node (0, 9)), respectively. Two local parts (c) and (d) in Fig. 4a are enlarged in Fig. 4c and Fig. 4d, respectively. In Fig. 4a and Fig. 4c, it is found that when the input current increases up to 0.225mA, the maximum temperature in one mesh segment reaches the melting point of Ag nanowire making the start point of the melting of mesh. For the following melting of the second mesh segment, the melting current decreases to the value of 0.217mA. With the melting propagation of mesh segment, the variation of melting current and voltage shows the repetition of three different trends as marked with arrows in Fig. 4c and Fig. 4d: (I) decrease of both melting current and voltage; (II) increase of both melting current and voltage; (III) decrease of melting current but increase of melting voltage. Finally, the melting of last mesh segment makes the open circuit of the mesh as shown in Fig. 4a. Here, the number of broken mesh segments n_b corresponding to the open circuit of mesh is only 89, which is about one half of the number of the overall mesh segments (i.e., 180) in the intact Ag nanowire mesh. Generally, the nanowire mesh during the whole melting process in this case keeps symmetric, in which the exception is attributed to the minor error during the numerical simulation. On the other hand, the mesh resistance in Fig. 4b increases with the melting propagation of mesh segment, which is independent of the trend of melting current.

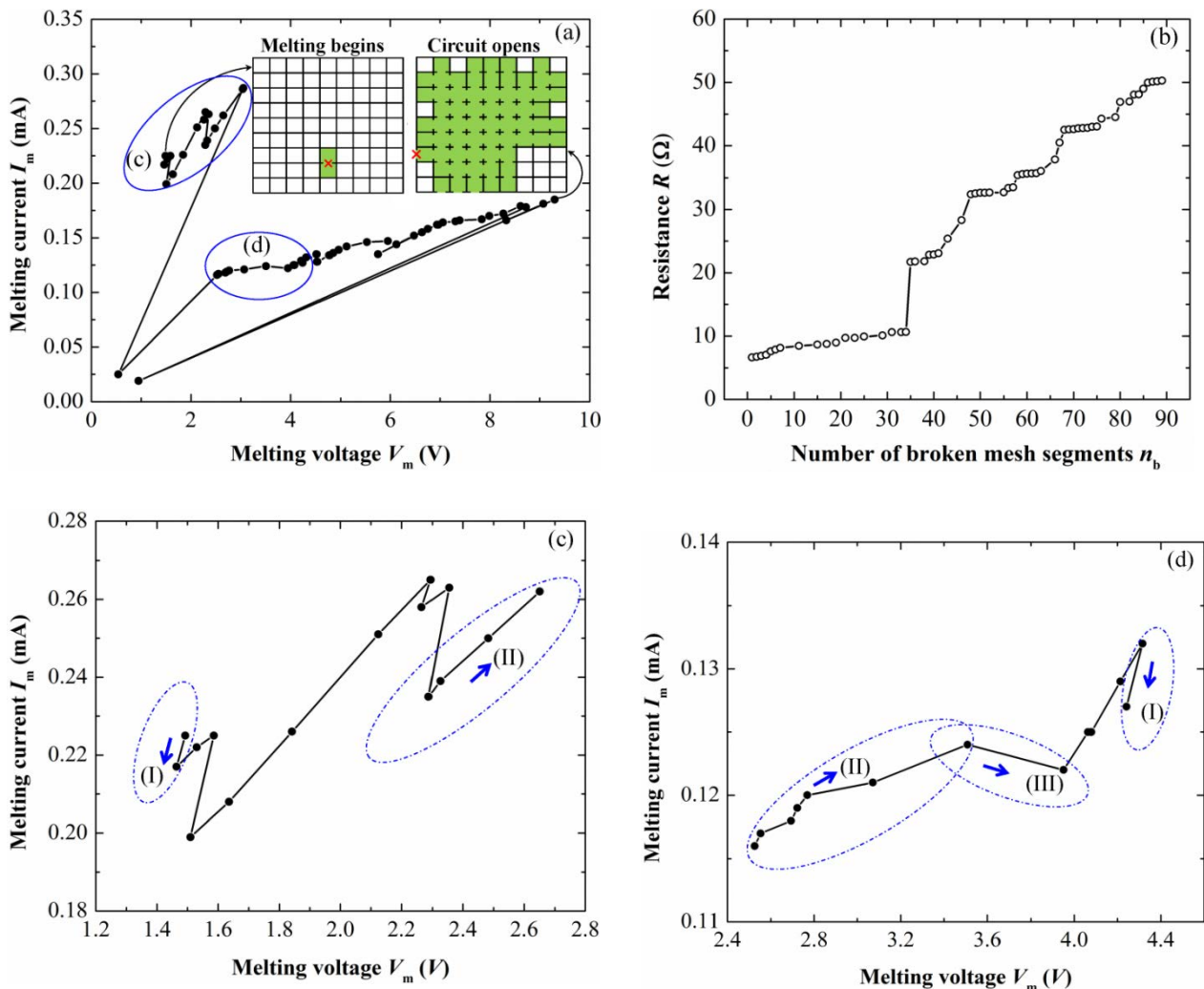


Fig. 4 Numerical melting of an Ag nanowire mesh structure

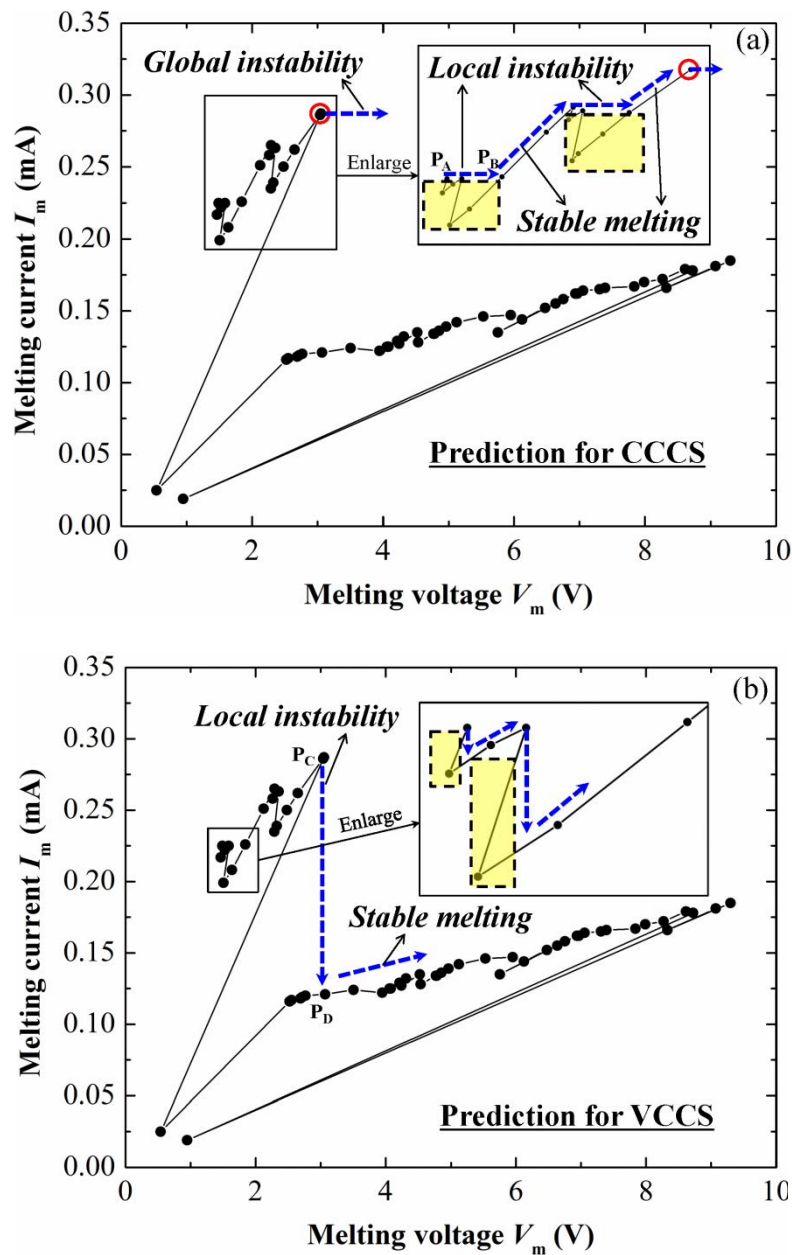


Fig. 5 Predicted experimental melting process of a system of an Ag nanowire mesh equipped with current source (CCCS: current-controlled current source; VCCS: voltage-controlled current source)

To explain this unique melting behavior of a mesh structure, the melting of an individual nanowire is discussed here to make comparison. The maximum temperature induced by Joule heating in the nanowire increases with increasing current. When the maximum temperature reaches to the melting point of the material, the nanowire will melt, and the melting process of an individual wire is finished. For the mesh structure, on the other hand, the maximum temperature in the mesh, occurring in some place of a mesh segment, initially increases with the increasing current, which is similar with that of the individual nanowire. When the maximum temperature reaches to the melting point of the material, the corresponding mesh segment melts. However, this is just the start point of melting in the mesh structure, and the mesh structure intrinsically takes a consecutive melting

process of large amounts of individual nanowires.

Basically, due to the limit of the properties of current sources, it is difficult to observe the trend of (I) in Fig. 4 (c) and (d) in which both melting current and voltage decrease. Consider a system composed of an Ag nanowire mesh and current source, the corresponding melting behavior can be predicted. As a representative illustration, Fig. 5 is given. For the mode of current-controlled current source (CCCS) in Fig. 5a, such regions with the decrease of current and the subsequent recovery (e.g., the area surrounded by dash rectangular) is difficult to be reproduced in experiment. The dashed arrows indicate the predicted variation of melting current and voltage during experimental melting process of the system. The rightwards dashed arrow means that at a constant current, several mesh segments melt simultaneously leading to the increase of resistance and therefore the increase of the voltage. This phenomenon is defined as *local instability*, which is a jump (e.g., from point P_A to point P_B in Fig. 5a) when compared to the melting current-voltage curve during numerical melting. The north east dashed arrow indicates that the increase of current is necessary for the further propagation of melting. This behavior is called *stable melting*. Moreover, the existence of the maximum melting current, marked by a circle in Fig. 5a, tells that if the input current is high enough, the mesh segments will melt simultaneously until the circuit of mesh is open. This phenomenon is denoted as *global instability*. On the other hand, for the mode of voltage-controlled current source (VCCS) in Fig. 5b, such regions with the decrease of voltage and the subsequent recovery (e.g., the area surrounded by dashed rectangular in the enlarged part) are difficult to realize experimentally. The dashed arrows indicate the predicted variation of melting current and voltage during experimental melting process of the system in a similar strategy with that for the mode of CCCS. There is the repetition of the vertical descent stage and the ascent stage until the circuit of mesh is open. The downwards dashed arrows indicate the vertical descent stages, where the melting of several mesh segments will happen simultaneously at a constant voltage, which shows local instability (e.g., the jump from point P_C to point P_D in Fig. 5b). The north east dashed arrows show the ascent stages, where the increase of voltage is requisite for the melting propagation, which shows stable melting. The only difference from that of CCCS mode is that there is no global instability for VCCS.

4. Conclusions

In the present work, the electrical breakdown of a metallic nanowire mesh induced by Joule heating is investigated by solving the corresponding electro-thermal problem, where the effect of electromigration is neglected for simplicity. A numerical computational program is developed to determine the temperature profile in the mesh, and the melting current triggering the melting of mesh segment. The structural melting of a metallic wire mesh is investigated by clarifying the variation of melting current with regard to the melting propagation of mesh segments. The melting behavior of a system of the mesh equipped with current source in real experiments can then be predicted, in which two modes of current source are discussed in detail. Local instability and stable melting will occur in spite of the mode of current source. Moreover, global instability only happens at the mode of current-controlled current source. This finding deepens the understanding of the electrical breakdown behavior of a metallic nanowire mesh, and may therefore contribute to the development of nanowire-based devices with high reliability.

Acknowledgements

The authors are grateful to be partly supported by Tohoku Leading Women's Jump Up Project for 2013 (J120000428) from the Ministry of Education, Culture, Sports, Science and Technology (MEXT) of Japan.

References

- [1] M.S. Dresselhaus, Y.M. Lin, O. Rabin, M.R. Black, G. Dresselhaus, Nanowires, in: B. Bhushan (Eds.), Springer Handbook of Nanotechnology (3rd edition), Springer-Verlag, Heidelberg, 2010, pp.119-168.
- [2] M. Kang, H. Park, S. Ahn, L. Guo, Transparent Cu nanowire mesh electrode on flexible substrates fabricated by transfer printing and its application in organic solar cells. *Solar Energy Materials & Solar Cells*, 94 (2010) 1179-1184.
- [3] J. Groep, P. Spinelli, A. Polman, Transparent conducting silver nanowire networks. *Nano Lett*, 12 (2012) 3138-3144.
- [4] H. S. Carslaw, J. C. Jaeger, *Conduction of heat in solids*, Clarendon, Oxford, 1959, pp. 149-151.
- [5] H. Tohmyoh, T. Imaizumi, H. Hayashi, M. Saka, Welding of Pt nanowires by Joule heating. *Scripta Mater*, 57(2007) 953-956.
- [6] H. Tohmyoh, S. Fukui, Manipulation and Joule heat welding of Ag nanowires prepared by atomic migration. *J Nanopart Res*, 14 (2012) 1116.
- [7] H. Park, A. Lilley, A. Alivisatos, J. Park, P. McEuen, Fabrication of metallic electrodes with nanometer separation by electromigration. *Appl Phys Lett*, 75 (1999) 301-303.
- [8] T. Taychatanapat, K. Bolotin, F. Kuemmeth, D. Ralph, Imaging electromigration during the formation of break junctions. *Nano Lett*, 7 (2007) 652-656.
- [9] Q. Huang, C. L., R. Divan, M. Bode, Electrical failure analysis of Au nanowires. *IEEE Transaction on Nanotechnology*, 7 (2008) 688-692.
- [10] J. Zhao, H. Sun, S. Dai, Y. Wang, J. Zhu, Electrical breakdown of nanowires. *Nano Lett*, 11(2011) 4647-4651.
- [11] M. Saka, Y. X. Sun, S. R. Ahmed, Heat conduction in a symmetric body subjected to a current flow of symmetric input and output. *Inter J Therm Sci*, 48 (2009) 114-121.
- [12] A. Mayoral, L. F. Allard, D. Ferrer, R. Esparza, M. Yacaman, On the behavior of Ag nanowires under high temperature: in situ characterization by aberration-corrected STEM. *J Mater Chem*, 21(2011) 893-898.
- [13] J. Xu, A. Munari, E. Dalton, A. Mathewson, K. M. Razeeb, Silver nanowire array-polymer composite as thermal interface material. *J Appl Phys*, 106 (2009) 124310.
- [14] X. Liu, J. Zhu, C. Jin, L. Peng, D. Tang, H. Cheng, In situ electrical measurements of polytypic silver nanowires. *Nanotechnology*, 19 (2008) 085711.